

Light-Switchable Hemithioindigo–Hemistilbene-Containing Peptides: Ultrafast Spectroscopy of the Z → E Isomerization of the Chromophore and the Structural Dynamics of the Peptide Moiety

N. Regner,^{†,#} T. T. Herzog,^{†,#} K. Haiser,[†] C. Hoppmann,^{‡,§} M. Beyermann,[†] J. Sauermann,[§] M. Engelhard,[§] T. Cordes,^{||} K. Rück-Braun,^{*,‡} and W. Zinth^{*,†}

[†]BioMolekulare Optik and Center for Integrated Protein Science at the Department of Physics, Ludwig-Maximilians University Munich, Oettingenstraße 67, 80538 Munich, Germany

[‡]Institut für Chemie, Technische Universität Berlin, Straße des 17. Juni 135, 10623 Berlin, Germany

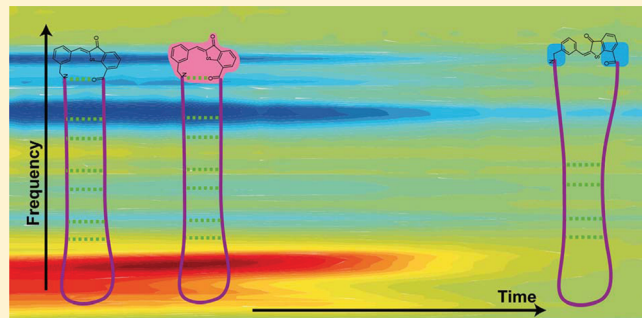
[§]Max-Planck-Institute for Molecular Physiology, Otto-Hahn-Straße 11, 44227 Dortmund, Germany

^{||}Molecular Microscopy Research Group & Single-Molecule Biophysics, Zernike Institute for Advanced Materials, University of Groningen, Nijenborgh 4, 9747 AG Groningen, The Netherlands

^{*}Leibniz-Institut für Molekulare Pharmakologie (FMP), Robert-Roessle-Straße 10, 13125 Berlin, Germany

S Supporting Information

ABSTRACT: Two hemithioindigo–hemistilbene (HTI) derivatives, designed to operate as structural switches in peptides, as well as two HTI peptides are characterized by ultrafast spectroscopy in the visible and the infrared. The two HTI switches follow the reaction scheme published for other HTI compounds with a picosecond excited state reaction ($\tau_1 \approx 6$ ps) and isomerization from Z to E with $\tau_2 = 13$ and 51 ps. As compared to the isolated chromophores, the isomerization reaction is slowed down in the chromopeptides to $\tau_2 = 24$ and 69 ps. For the smaller peptide containing 6 amino acids, the structural changes of the peptide moiety observed via the IR spectrum in the amide I band follow the isomerization of the molecular switch closely. In the larger cyclic chromopeptide, containing 20 amino acids and mimicking a β -hairpin structure in the Z-form of the chromophore, the peptide moiety also changes its structure during isomerization of the chromophore. However, the IR spectrum at the end of the observation period of 3 ns deviates significantly from the stationary difference spectrum. These signatures indicate that strong additional structural changes, e.g., breaking of interchain hydrogen bonds, also occur on longer time scales.



1. INTRODUCTION

Protein folding as a major biological process is still far from a quantitative understanding.^{1,2} The fundamental transition from the unordered “random coil” arrangement of an amino acid chain into the functional active “native protein” with a well-defined structure is a topic of numerous investigations.^{1,2} Moreover, conformational changes in proteins associated with protein domain motion are nowadays widely recognized as the bridging element between structure and function.³

The inherent problem of protein folding and protein motion concerns the intrinsic large number of degrees of freedom and the wide time range involved. It spans from the subpicosecond time-scale for elementary molecular processes, such as bond-rotation or hydrogen bond formation/rupture^{3–11} to the completion of a folding process that may take much longer than seconds.^{12,13} Both facts prevent the detailed computational simulation of folding processes even by the most elaborate state-of-the-art-techniques. Coarse-grain ap-

proaches,¹⁴ which combine several atoms into functional parts, may pave the way to simulations of large peptides on time scales up to milliseconds. Another promising strategy to gain more insight into the basics of folding processes and conformational changes focuses on systems with reduced size such as small peptides. Here the transition between different conformational states can be induced by external events, e.g., light-activation or temperature changes. In such model systems, folding as well as conformational changes may be completed within microseconds, a feature that, combined with the small size of the peptides, may allow one to perform high-quality molecular dynamics simulations of the complete folding process with sufficient statistical significance. A combination of simulations of peptides with results from experimental

Received: January 31, 2012

Revised: March 14, 2012

Published: March 16, 2012



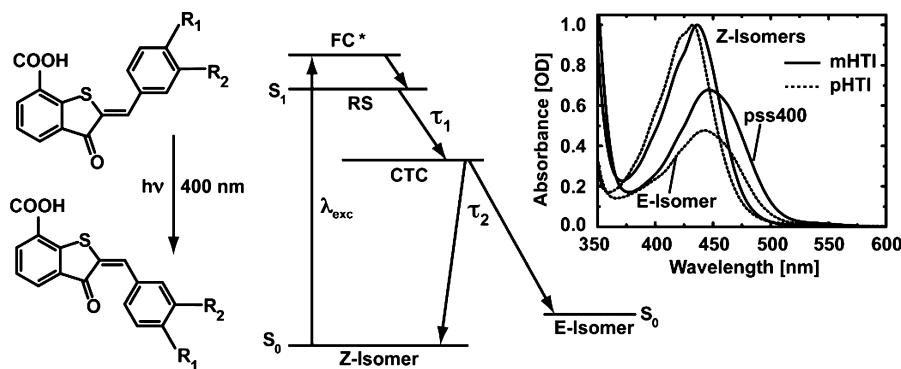


Figure 1. Schematic presentation of the HTI-structures reached upon isomerization (left). Different substitutions (R_1 and R_2) have been used for the molecules studied in this publication. Reaction scheme of HTI for the $Z \rightarrow E$ isomerization deduced from previous investigations (center). Light absorption populates the Franck–Condon region (FC^*). The reaction proceeds via the relaxed state (RS) and a state with charge transfer character (CTC). Right: Absorption spectra of the two HTI isomers pHTI (solid curve) and mHTI (dashed curve). For mHTI, the spectrum of the photostationary state pss400 is shown, where illumination around 400 leads to a concentration of ca. 70%.

investigations of structural dynamics, e.g., by using transient IR spectroscopy can hence lead to a deeper insight into the mechanisms of peptide folding.¹⁵

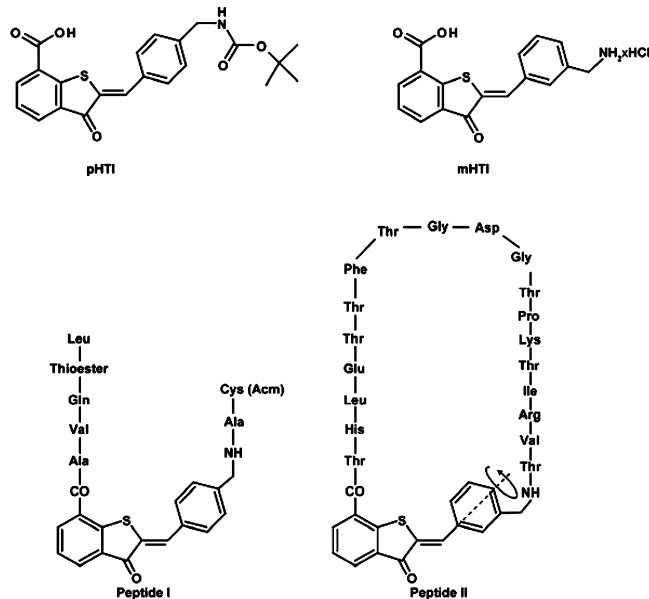
Direct access to the fastest molecular processes of peptide folding has been obtained by introducing light-switchable peptides, where the isomerization reaction of a photochromic molecule is used to trigger folding or unfolding reactions.¹⁶ The light-switchable chromophore is directly incorporated into the amino-acid sequence as a backbone element. Chromophore-induced switching has also been used for enzymatic reactions,^{17–19} for the manipulation of the biological activity of cells,^{20–22} to activate ion transfer channels in neurons,²³ helping to control neuronal activity in higher organisms, for disaggregation of amyloid-like structures or to activate specific drugs upon light exposure.^{24,25}

One of the most widely used photoswitches is azobenzene, a compound that is known to combine high switching speed (a typical time constant for the *cis* to *trans* photoisomerization of azobenzene is 300 fs) with strong mechanical driving forces and high photochemical quantum efficiencies in the range of 50% (for the *cis* to *trans* reaction).²⁶ Azobenzene and its derivatives, however, have severe disadvantages for a number of applications: Most derivatives require illumination in the ultraviolet, the photochemically active $n\pi^*$ transition has only a small cross section ($1000\text{--}2000 \text{ L mol}^{-1} \text{ cm}^{-1}$), and many azobenzene compounds are known to be susceptible to cellular environments or to be harmful for a living organism.^{27,28}

Among the various photochromic compounds (e.g., azobenzenes, fulgides, fulgimides,²⁹ diarylethenes,³⁰ chromenes^{31,32}), the recently established family of hemithioindigo–hemistilbene (HTI) shows properties that make HTI derivatives interesting candidates for peptide switching: HTI has visible absorption bands allowing optical switching. It has good photostability, and the reaction dynamics can be influenced/tuned by chemical substituents at various positions within the molecule.^{33–38} The absorption band of the Z-isomer of HTI compounds around 430 nm has extinction coefficients above $10\,000 \text{ L mol}^{-1} \text{ cm}^{-1}$. The quantum efficiencies are reasonable. Typical values for the $Z \rightarrow E$ reaction are in the 10–20% range.³⁷ Furthermore, a reaction scheme for HTI (see Figure 1) is well established, and it could already be shown that HTI can be used for switching the conformation of peptides when the molecule is incorporated into the backbone of small peptides.³⁷

In order to supplement and to complete information on the mechanisms of HTI-mediated ultrafast reaction dynamics, two novel HTI peptides (Scheme 1) of different size and structure

Scheme 1. Molecular Structures of Chromophores and Peptides Studied in This Paper^a



^aThe dashed line in the scheme of Peptide II represents the additional degree of freedom introduced by substitution at the meta position.

were analyzed in this paper in more detail. Both peptides are derived from proteins involved in cell signaling. The amino acid sequence of linear peptide I stems from a loop region of the sensory rhodopsin II-transducer complex involved in transmembrane signal transfer.³⁹ Future experiments are designed where HTI will be used as a light activated trigger in transmembrane signal transfer. Cyclic Peptide II is derived from one of the best-understood examples among PDZ-organized signaling complexes: the neuronal nitric oxide synthase (nNOS) β -finger-syntrophin complex.⁴⁰ To trigger structural changes in the peptide we use ultrashort light pulses at 400 nm inducing the $Z \rightarrow E$ photoisomerization of the HTI chromophore. Probing light in the visible/near-ultraviolet allows us to observe the photoisomerization of the chromophore. Probing

in the mid-IR monitors the dynamic processes of the peptide moiety. All HTI samples follow the same reaction scheme with decreased isomerization speed in the two peptides. The absorption transients in the mid-infrared point to electronic coupling between the excited chromophore and peptide groups and display changes in the peptide structure during HTI isomerization. For the larger cyclic peptide II, the IR absorption spectrum does not reach its stationary form within the observation period of 3 ns. Presumably, the conformational freedom of the mHTI photoswitch used in this peptide prevents the completion of all structural changes in rapid and force driven reactions. Apparently, the peptide adjusts in slower allosteric steps to the new structure of the E isomer of the HTI switch.

2. MATERIALS AND METHODS

Sample. Peptide I was manually synthesized by solid phase peptide synthesis using Boc-strategy (for a detailed description, see ref 41). The peptide was assembled on a Leu-thioester Pam resin. After having coupled Ala, the N-terminal protecting group was cleaved by treating the resin with trifluoroacetic acid (TFA) and subsequently with *N,N*-diisopropylethylamine (DIEA) for neutralization. The amino acid analogue of HTI (3 equiv in the first coupling; 2 equiv in the second coupling) was coupled to Ala using *O*-benzotriazole-*N,N,N'*-tetramethyl-*U*-ronium-hexafluoro-phosphate (HBTU) activation. After assembling the full length peptide, peptide I was cleaved from the resin by hydrogen fluoride⁴¹ and purified by high-performance liquid chromatography (HPLC) using a semi preparative C18 column. By electrospray ionization (ESI) mass spectrometry, a mass of 1042.5 Da (theoretical value $[M+H]^+$ = 1042.3 Da) was determined.

Peptides II and IIa were prepared on 2-chlorotrityl resin using standard protocols and Fmoc chemistry by essentially following a recently published procedure.⁴⁰ The Fmoc-protected HTI building block was coupled in 2.5-fold excess manually by HBTU and DIEA (1:1) in dimethylformamide (DMF). The synthesis was carried out with the pseudoproline Fmoc-VT-OH. Cleavage of the fully protected peptides was accomplished with dichloromethane (DCM)/acetic acid (AcOH)/tetrafluoroethylene (TFE) (3:1:1) for 1 h. The linear peptides were cyclized by applying benzotriazol-1-yl-oxy-tritypyrrolidinophosphonium hexafluorophosphate (PyBOP), DIEA, and DMF in DCM as solvent. For the final deprotection, the cyclized peptides were treated with TFA, water, and phenol, and the cyclic peptides were finally purified by reversed-phase HPLC (RP-HPLC; ESI mass spectrometry: peptide II $[M+2H]^{2+}$ calc. 1175.5372 (monoisotopic), found 1175.5333; peptide IIa $[M+2H]^{2+}$ calc. 1183.5347 (monoisotopic), found 1183.5370). Irradiation of the thermodynamically stable Z form at 415 nm in methanol at pH 5.5 ($c = 0.56 \times 10^{-4}$ M) yielded a photostationary state (pss) of the E form (72% E content), and irradiation at 514 nm gave the pss of the Z form (97% Z content). During repeated photochemical interconversion at 415 and 514 nm, precipitation or photobleaching was not observed (see Supporting Information, Figure SI-1). The different samples were dissolved in perdeuterated methanol (CD_3OD , Merck, purity 98.9%) at concentrations between 1 and 3 mM for transient visible and transient IR-experiments, respectively.

Steady-State Absorption. UV/vis spectra were recorded using Perkin-Elmer Lambda 750 and Lambda 19 spectrophotometers, and spectra in the IR were recorded using a Fourier

transform infrared (FTIR) spectrometer (Model IFS 66, Bruker). The IR-spectra were taken with CaF_2 flow cells with an optical path length of 190 μm . The photoisomerization was induced by illumination of the sample within the spectrophotometer housing via optical fibers.

Ultrafast Absorption Spectroscopy. The time-resolved experiments were performed using femtosecond pump pulses in combination with suitably delayed probing pulses at different wavelengths. The time-resolved experiments are based on a Ti-sapphire laser-amplifier system (Spitfire Pro, Spectra Physics) operated at a central wavelength of ~ 800 nm, pulse durations of ~ 100 fs, and a repetition rate of 1 kHz. The excitation (pump) pulses in the near UV at 400 nm were generated by frequency doubling the fundamental of the laser in a β -barium borate (BBO) crystal. Every second pump pulse was blocked by a mechanical chopper in order to improve referencing when recording the pump-induced absorption changes of the sample. The sample solutions were investigated in flow cells and continuously exchanged by a peristaltic pump at flow rates sufficient to exchange the sample volume in the laser focus between two consecutive laser pulses. All time-resolved transient absorption experiments (TA) were performed on samples at photo stationary conditions, with a significant excess (>97%) of the studied Z-isomer. For this purpose, the sample solution was illuminated with a cold light source (KLC2500, Schott, Mainz) filtered by a 3 mm-thick GG495 (Schott).

Time-Resolved Experiments in the UV/Vis. The pump pulses in the UV/vis experiments had an excitation energy of ~ 500 nJ (beam diameter in the sample $d_{pump} = 150$ μm). Probing of the induced absorption changes was performed by a suitably delayed white light continuum generated in CaF_2 ⁴² (~ 350 –700 nm, beam diameter in the sample $d_{probe} = 50$ μm) with polarization at the magic angle. The spectrum of the transmitted probing light was measured by a multichannel detection system: The probe pulses were dispersed by a concave grating (Zeiss, focal distance at 200 nm 111 mm, groove number 320 mm^{-1} , blazed at 225 nm) on a NMOS linear image sensor (Hamamatsu 14-S3902-512Q in combination with TecS DZA-S3901-4 1 M preamplifier electronic). The sample solution was continuously pumped through a flow-cell with fused-silica windows (optical path length 0.5 mm). The data points at certain delay times between pump and probe were measured with four repetitive scans and with 1000 exciting laser shots per data point. Transient background signals from the pure solvent were weighted and subtracted from the sample signal. The delay time of zero of all individual probe wavelengths was determined by a dispersion correction based on a Sellmeier fit.⁹

Time-Resolved Experiments in the Mid-IR. The experimental setup for the visible pump and infrared probe experiment has already been described in detail.⁴³ The main difference in the present work is the use of a Spitfire Pro laser system as the source for the femtosecond light pulses. The excitation energies vary between 1 and 2 μJ for the pure photoswitch and photoswitch-peptide systems, respectively. The spot diameter of pump and probe pulses at the sample location were 220 and 90 μm , respectively. The polarization of the pump was set to magic angle with respect to the probe light. The mid-IR probing pulses were generated using nonlinear frequency conversion (spectral width ~ 200 cm^{-1} , duration ~ 150 fs).⁴³ The transient absorption change was recorded by a 32-channel mercury-cadmium-telluride detector array in combination with a spectrograph (Acton Research Corp-

ration, Spectra Pro-300i). To cover the entire spectral range from 1450 to 1750 cm^{-1} , IR probe pulses centered at five different spectral positions were used.

3. RESULTS

In the present paper, two different HTI chromopeptides with linear and cyclic structure were synthesized and investigated (Peptides I and II; see Scheme 1). The phenyl ring of the HTI switching unit can be substituted in the para or meta position (R_1 and R_2 , respectively) to form either an amino acid or chromopeptide (see Figure 1 for chromophore structure; see Scheme 1 for HTI chromopeptides). Photoisomerization of HTI occurs around the central double bond leading to the two isomers Z and E with pronounced differences in their absorption spectra (see Figure 1, right side). The Z-form is thermally stable, while the E form reconverts at room temperature to the Z-form on the time scale of hours depending on the specific substitution.^{33,34,38} In addition, the two isomers can be interconverted by light at appropriate wavelengths.³⁸

A reaction model for the $Z \rightarrow E$ photoisomerization is presented in the central part of Figure 1.⁴⁴ After excitation of the Z-isomer of an HTI compound into its lowest excited electronic state with light around $\lambda_{\text{exc}} = 400 \text{ nm}$, one finds initial absorption transients in the subpicosecond time scale that are related to the motion away from the initially excited Franck–Condon region (FC^*) via fast solvation processes. On the time scale of a few picoseconds (time constant τ_1), HTI in the relaxed state (RS) undergoes further rearrangements of its electronic structure. Presumably the molecule changes its electronic structure and acquires a state with some charge transfer character (CTC).⁴⁵ After completion of this reaction, the HTI molecule is still in an electronically excited state. It is on a longer time scale (time constant τ_2) that this CTC state decays into the electronic ground state of the product, the isomerized E form, or the starting Z form. It has been found that this model describes the photoisomerization for a number of differently substituted HTI molecules well. The values of the two time constants τ_1 and τ_2 depend, however, on substitution.^{35,36} Especially, the lifetime τ_2 strongly changes with substitution of the stilbene/hemithioindigo part of the HTI molecule. Substitution on the stilbene part of the molecule quantitatively obeys the Hammett relation with electron-donating/withdrawing groups increasing/decreasing the reaction speed. An inverse behavior was found for substitution at the hemithioindigo part. The influence of substitution is hence consequently reduced when electron donating or withdrawing groups are not directly fused to HTI but are linked via a methylene spacer. Such an approach has been used in the design of the two peptides.

In the following experiments, four HTI compounds and chromopeptides have been investigated. (i) The HTI switch pHTI with $R_1 = \text{CH}_2\text{--NH}_3^+$ and $R_2 = \text{H}$ (see Figure 1 and Scheme 1). In this compound, the connecting C-terminus of a peptide may be attached at the para position to the stilbene part of the HTI. (ii) Peptide I contains six amino acids in two short chains linked to the pHTI (see Scheme 1). The CH_2NH group is connected to the dipeptide Cys-Ala. The N-terminus of Ala-Val-Gln-Thioester-Leu binds to the carbonyl group attached to the hemithioindigo part of the switching molecule. The sequence chosen represents a loop region connecting two transmembrane helices from the photoreceptor complex comprising sensory rhodopsin II and its cognate transducer.

A switch at this position might be taken as a trigger for transmembrane signal transfer. (iii) The second switching unit is mHTI, which has $R_1 = \text{H}$ and $R_2 = \text{CH}_2\text{--NH}_3^+$ (see Figure 1). A consequence of the meta functionalization of the phenyl ring in the mHTI switching unit is an increased conformational freedom. This has been observed previously for related azobenzene amino acids.^{10,46} (iv) Peptide II (see Scheme 1) is derived from the β -finger structure of nNOS (30 amino acid residues), which is involved in binding to syntrophin, thereby mediating the membrane association of nNOS to skeletal muscles. This process induces the production of the second messenger nitric oxide (NO) for muscle contraction.^{22,40} The two termini of the peptide chain are connected to the mHTI-switch, forming a cyclic molecule. Hereby the C-terminus of the amino acid chain is linked via the CH_2NH group to the stilbene part of mHTI in meta position. The use of mHTI opens additional conformational freedom since rotations around the symmetry axes (see dashed line in Scheme 1) are possible and lead to different structures of the Peptide II. The N-terminus is attached to the carboxyl group of the hemithioindigo group of mHTI. Photoswitching of the HTI moiety is expected to alter the conformation of peptide II and to disturb the binding of the peptide ligand to syntrophin.^{22,40}

Stationary Spectroscopy. The visible and near UV absorption spectra of the Z- and E-isomers of pHTI (solid curve) and mHTI (dashed curve) are shown in the right part of Figure 1. The absorption peak of the Z-isomer is around 430 nm. The absorption of the E-isomer is weaker by a factor of 2, and the peak is red-shifted to 450 nm. It should be noted that both HTI peptides studied in this paper exhibit very similar absorption spectra.

The stationary IR spectra (normalized) of the para-substituted samples are shown in Figure 2. The IR absorption

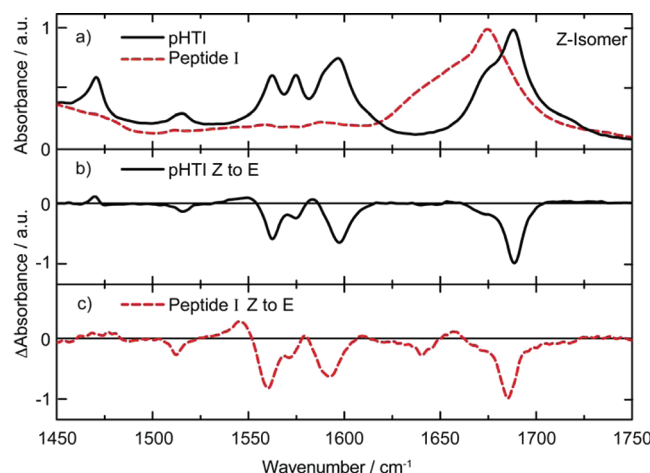


Figure 2. Stationary IR spectra of the Z-isomer of pHTI and Peptide I (a). Stationary absorption difference spectra for the $Z \rightarrow E$ transition of pHTI (b) and Peptide I (c).

of the chromophore pHTI in its Z-form (black solid curve) shows an absorption band between 1650 and 1700 cm^{-1} due to the different C=O groups. The pronounced narrow peak at 1680 cm^{-1} is due to the carbonyl group at the central five-membered ring, whereas the broader shoulder can be related to the C=O vibration of the COOH group. Further absorption bands of the pHTI visible between 1550 and 1600 cm^{-1} can be assigned to CC-stretching modes of the aromatic system. The

change in IR absorption upon photoisomerization of pHTI is shown in Figure 2b. One finds a strong reduction of the C=O absorption band of the cyclic carbonyl group. In addition, the three bands at 1560, 1575, and 1595 cm⁻¹ decrease as well as the absorption of the weak band found at 1520 cm⁻¹. Apparently, the isomerization of the pHTI molecule changes not only the overall structure of the molecule but also the observed vibrations. It should be noted that the absorption changes are predominantly negative, i.e., in the E-isomer the absorption cross sections are reduced as compared to the Z-isomer. Newly formed bands are weaker than the original bands of the Z-isomer, or have frequencies outside the displayed spectral window, a fact that prohibits one from observing the formation of the E-photoproduct in time-resolved experiments via (positive) marker bands of the HTI E-isomer.

The normalized IR-absorption spectrum of Peptide I is shown as a dashed curve in Figure 2a, normalized to its peak at 1675 cm⁻¹. The absorption between 1600 and 1700 cm⁻¹ is dominated by features from amide I vibrations. The peak of the amide I absorption is at 1675 cm⁻¹ in a range known for weak or negligible hydrogen bonding of the amide group; an extended shoulder at lower frequencies indicates that a minor fraction of amide groups are hydrogen bonded.⁴⁷ Weaker absorption features (e.g., shoulder extending to >1700 cm⁻¹ and some modulation in the 1550 cm⁻¹ range) can be related to the presence of the pHTI chromophore (based on knowledge of the chromophore spectrum of Figure 2a). The absorption difference spectrum (Peptide I) recorded after steady-state illumination is shown in Figure 2c. It largely resembles the absorption differences of the pure chromophore pHTI (Figure 2b). Additional features are a dispersive signature at 1650 cm⁻¹ and an absorption increase at 1540 cm⁻¹. While the absorption spectrum of Peptide I is dominated by the peptide part, its stationary difference spectrum is mainly determined by the chromophore bands. Apparently, the isomerization of the chromophore to the E form only leads to small structural changes in the peptide part. The dispersive feature at 1650 cm⁻¹ indicating a weak blue shift in the amide range can be taken as a result of reduced H-bonding of amide groups or from small changes in the peptide arrangements.

Figure 3a shows the stationary IR spectra of mHTI (solid curve) and Peptide II (dashed curve, scaled). The absorption spectrum of mHTI displays strong absorption bands from the two C=O groups and contributions from the C=C ring modes between 1550 cm⁻¹ and 1620 cm⁻¹. The absorption spectra of the chromophores pHTI and mHTI (Figures 2a and 3a) as well as the difference spectra upon photoisomerization (Figures 2b and 3b) are similar. However, the IR absorption spectrum of Peptide II differs strongly from that of Peptide I. It is dominated by the amide I absorption band peaking at 1645 cm⁻¹. An extended shoulder is seen between 1650 and 1700 cm⁻¹. Toward lower frequencies (<1600 cm⁻¹) Peptide II shows weak and featureless absorption. Absorption bands from the mHTI chromophore are not visible. Apparently the absorption of the large number of amino acids in Peptide II completely covers the absorption of the mHTI chromophore. Position and shape of the amide I band indicate that in Peptide II many amide groups show strong interstrand hydrogen bonds, as is expected for a β -hairpin structure.⁴⁷

The absorption change induced by Z- to E-isomerization of the mHTI chromophore of Peptide II displays a strong absorption change with a negative band at 1642 cm⁻¹ and a broader induced absorption above 1650 cm⁻¹. Around 1680

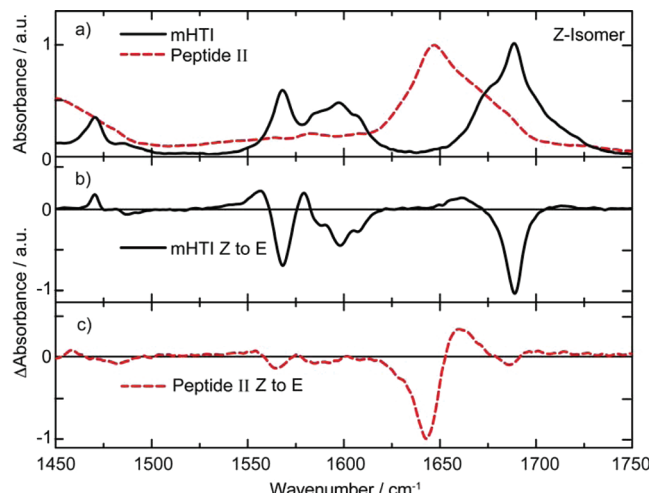


Figure 3. Stationary IR spectra of the Z-isomer of mHTI and Peptide II (a). Stationary absorption difference spectra for the Z → E transition of mHTI (b) and Peptide II (c).

cm⁻¹, one observes some absorption decrease. Weak absorption features are visible at locations of the dominant absorption difference bands of the chromophore mHTI, i.e., at 1680 cm⁻¹ (C=O), 1550–1600 cm⁻¹ (C=C). The stationary absorption difference clearly indicates that pronounced changes occur in the peptide moiety. The decrease at 1643 cm⁻¹ and the increase at higher frequencies can be interpreted as a significant change in the number and type of hydrogen bonds being involved in the antiparallel β -type peptide structure, thereby indicating that a certain fraction of the β -hairpin structure is disassembled in the E-form.

Comparable results were obtained for the assembling of an antiparallel β -type structure of a peptide ligand containing an azobenzene photoswitch in D₂O buffer upon trans-to-cis photoisomerization⁴⁰ and for another azobenzene containing a β -hairpin peptide in d₄-methanol.^{8,48} For a related FTIR study of the secondary structure of peptide II in d₄-methanol (*c* = 0.1 mM), Peptide IIa was also prepared, containing tyrosine instead of phenylalanine in the peptide backbone close to the Gly-Asp-Gly turn region (see Scheme 1), since the tyrosine side chain has a relatively strong absorption band (C-C stretching vibration of the aromatic ring) at 1515 cm⁻¹, which is sensitive to structural modifications.⁴⁹

FTIR spectra of peptide II in comparison to the modified Peptide IIa, containing tyrosine, are shown in the Supporting Information for the pure Z forms, the E forms in the pss, as well as the Z-E difference spectra (see Supporting Information: Figure SI-3 to Figure SI-5). In these studies, the IR spectrum of the Z form of peptide II in d₄-MeOH is also characterized by an amide I band at approximately 1646 cm⁻¹. In addition a characteristic shoulder is observed at 1684 cm⁻¹. This shoulder may originate from the high frequency band of an antiparallel β -sheet structure or from the absorption of the mHTI chromophore. A decrease of this amide I absorption is observed upon photoisomerization to the E form in the pss. In the E-Z IR difference spectrum the negative signals at 1645 and 1687 cm⁻¹ indicate a loss of antiparallel β -sheet structure. Similar results were obtained for peptide IIa containing tyrosine instead of phenylalanine. In addition, second-derivative spectra were used for peak positioning of the IR bands of Peptides II and IIa. In both peptides, the band of the side chain of glutamic

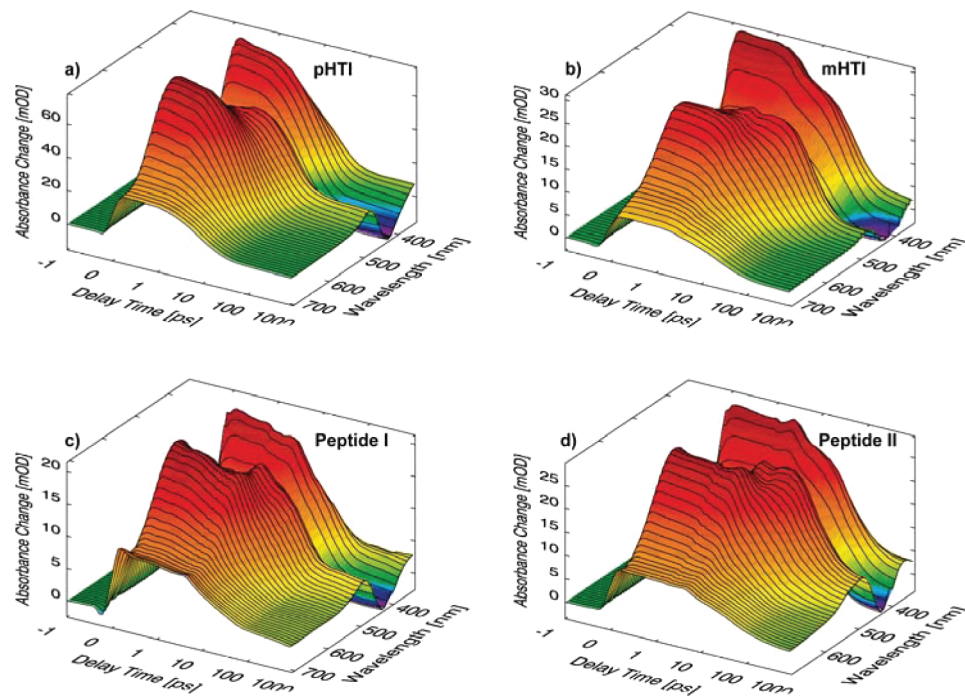


Figure 4. Overview of the transient absorption data recorded for the four HTI samples with probing wavelengths in the visible spectral range.

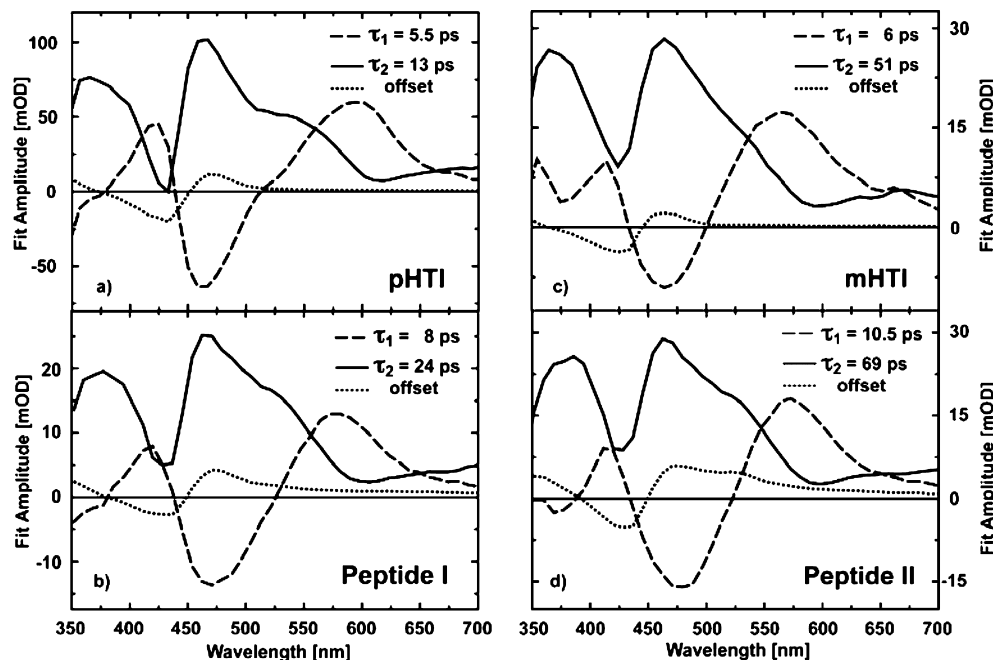


Figure 5. DAS deduced from a multiexponential fit of the visible absorption data with the time constants given in Table 1.

acid at 1563 cm^{-1} moves to lower wavenumbers, whereas the side chain of aspartic acid at 1583 cm^{-1} shows only a marginal shift, and the tyrosine band at 1515 cm^{-1} is not altered. The data indicate that, in the proximity of glutamic acid, conformational alterations are observable upon $Z \rightarrow E$ photoisomerisation. However, the loop region where the tyrosine and the aspartic acid are located remains essentially unchanged. In conclusion, the FTIR studies with Peptides II and IIa confirm structural modifications between the two strands of the antiparallel β -sheet, presumably by an alteration of the hydrogen bonding. Obviously, upon photoisomerization

the number of hydrogen bonds decreases, resulting in a melting of the antiparallel β -sheet structure.

Ultrafast Absorption Transients in the Visible. A time-resolved investigation of HTI-amino acids and chromopeptides in the visible spectral range gives information on the electronic transition of the molecular switches. However, no direct information on the peptide moieties is obtained since the amino acids do not absorb in the investigated spectral range. The results qualitatively reproduce those obtained from HTI-molecules studied earlier and sketched in Figure 1.^{37,38,44} An overview of the absorption transients is given in Figure 4. Examples for time dependence (times >1 ps) at selected

probing wavelengths are given in Supporting Information, Figure SI-6. For all four molecules, we observe a very fast transient in the 100 fs range. This process represents a transition away from the FC^* . Since this transient is not related to structural dynamics of the peptide moiety, we will not consider the process in the context of this paper. For a detailed analysis of the dynamics of all four HTI compounds (two HTI switches and two HTI chromopeptides), we use multi-exponential global fitting, which results in time constants in the picosecond to nanosecond range, and in the corresponding amplitudes, the decay associated spectra (DAS). For all four samples, there is a picosecond transient that can be fitted with a time constant in the range of $\tau_1 = 5.5$ to 10.5 ps. Also the DAS related to this process (see Figure 5, dashed curves) are very similar. This 5.5 ps process is related to changes in the excited state absorption and the stimulated emission spectrum, which point to molecular motions on the excited state potential energy surface. The similarity of the DAS of the molecules studied here with those from previous publications⁴⁴ indicate that the same molecular processes occur in HTI molecules: with 5.5 ps, the electronic structure evolves leading to a state with stronger charge separation.

At later times we observe for pHTI a strong change in absorption with a time constant of $\tau_2 = 13$ ps. This transient is related to strong absorption changes caused by the decay of the broad excited-state absorption and by a partial recovery of the absorption of the initial Z-isomer (see Figure 5a). Afterward, one finds indications for a transient absorption change in the 500 ps range with very small amplitudes. At the end of the observation period, the absorption changes can be assigned to the formation of E-isomer (dotted curve in Figure 5a): the final spectrum shows some decrease in the range of predominant Z-absorption as well as an absorption increase of the range with exclusive E-isomer absorption >475 nm. The absorption changes (time constant and amplitudes) show that the $\tau_2 = 13$ ps component is related to the decay of the excited electronic state, i.e., with the reformation of the ground-states of the initial Z-isomer and the photoproduct (E-isomer).⁴⁴ The very weak absorption changes in the 500 ps range mentioned above can be tentatively assigned to small structural rearrangements of the isomerized molecules in the solvent cage or to processes caused by a small population of triplet state molecules.⁴⁵

The transient absorption properties of Peptide I (see Figure 5b) are very similar but exhibit some differences: The time constant τ_2 is increased to 24 ps. The remaining absorption change at the end of our observation period exhibits the features related to the formation of the E-isomer. In addition, it shows a broad shoulder of induced absorption in the red. Apparently, the attached peptide leads to a slowing down of the decay of the excited electronic state and the isomerization rate of the HTI chromophore. Slowing down of internal conversion (time constant τ_2) could be due to the increased friction that acts upon the isomerization motion of the Peptide I in the viscous solvent. The extended red wing absorption found at late times in Peptide I can be related to a mechanical strain between peptide and chromophore persisting at the end of our observation time.

The absorption transients related to the decay of the excited electronic state of the compounds mHTI and Peptide II are slower than those of the pHTI compounds (mHTI: $\tau_2 = 51$ ps, Peptide II, $\tau_2 = 69$ ps). This behavior goes in line with previous investigations, showing that molecules with electron donating

groups at the meta-position exhibit smaller acceleration of the S_1 decay than molecules with substitutions in para-position (see Figure 4). Again, the peptide reacts slower than the isolated switch. The absorption offset at the end of the observation time shows for both mHTI samples the dispersive shape around 430 nm, which results from the decrease of Z- and the increase in E-isomer concentration (see Figure 5c,d). For Peptide II, there is an additional peak around 530 nm and an extended wing throughout the whole visible range. This feature may be seen again as a signature of a long lasting force (strain) between the isomerized chromophore and a not yet relaxed peptide or as an indication for the presence of an additional intermediate structure in Peptide II, not relaxing within the 2 ns time window studied here.

Transient IR Spectroscopy. More detailed information on reaction dynamics and the related structural changes in the peptide moiety is expected from probing the absorbance changes in the mid-IR. The time constants found here are similar to those observed when probing in the visible spectral range. In Figures 6–8, we show absorption difference spectra taken at certain delay times for the different pHTI and mHTI compounds.

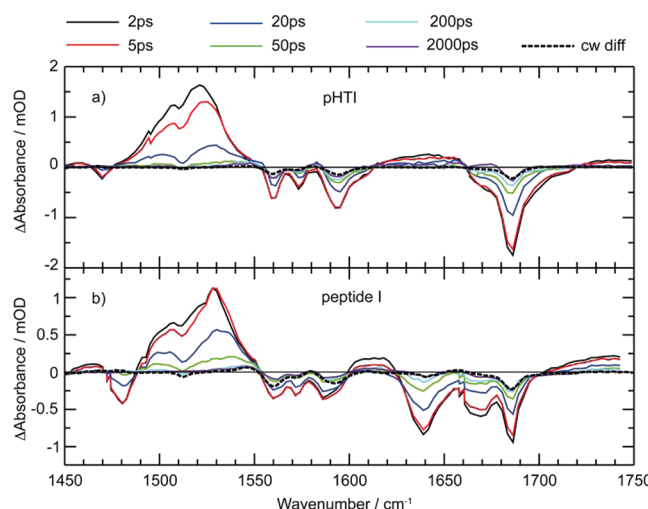


Figure 6. Transient absorption spectra recorded for the delay times given in the upper part of the figure for pHTI (a) and Peptide I (b). The dashed curves give the stationary difference spectra, scaled to fit the amplitudes of the transient absorption change of the band around 1685 cm^{-1} at late delay times.

pHTI. At early times ($t_d = 2$ ps), one observes a strong decrease in absorption at all positions where the Z-isomer of pHTI absorbs (see Figure 6a, in regions of $\text{C}=\text{C}$ and $\text{C}=\text{O}$ absorption). In addition, a strong band of increased absorption appears between 1475 and 1530 cm^{-1} . This band shows a dip at 1510 cm^{-1} , apparently due to the absorbance decrease of the ground-state band of the Z-isomer located here. Another absorption increase is found between 1600 and 1660 cm^{-1} . At higher frequencies, there is the bleach from the ground state $\text{C}=\text{O}$ band. Toward later delay times, the amplitudes of the absorption changes decrease, and at very late delay times the stationary absorption difference spectrum is reached (see Figures 6a and 7a). The analysis of the time dependence shows that the changes in the IR-spectrum can be described with similar time constants as those found above in the visible spectral range. The recovery of the ground state absorption

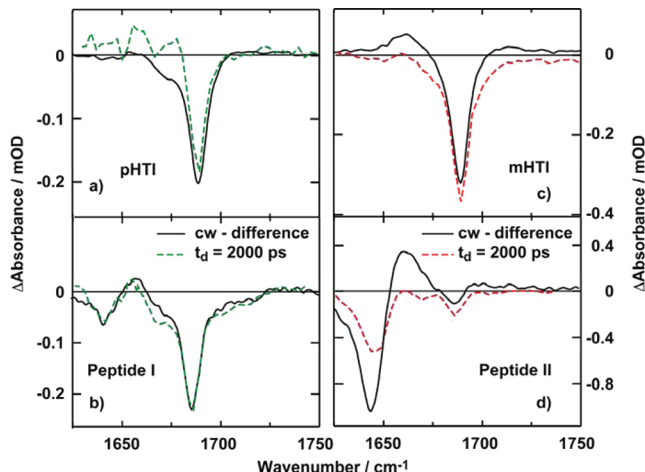


Figure 7. Transient absorption spectra recorded at a delay time of 2000 ps (dashed) and stationary absorption difference spectra (solid) recorded for pHTI (a), Peptide I (b), mHTI (c), and Peptide II (d).

bands occurs predominantly with the time constant $\tau_2 = 12.5$ ps (see Table 1). The induced absorption bands around 1530

Table 1. Time Constants Deduced from a Multiexponential Analysis of All Transient Absorption Data

R	$\tau_1^{\text{VIS}}/\text{ps}$	$\tau_2^{\text{VIS}}/\text{ps}$	$\tau_1^{\text{IR}}/\text{ps}$	$\tau_2^{\text{IR}}/\text{ps}$
pHTI	5.5 ± 1.1	13 ± 2.5	4 ± 1.2	12.5 ± 3.5
Peptide I	8 ± 3.2	24 ± 7	5.5 ± 1.5	23 ± 7
mHTI	6 ± 1	51 ± 5	3.5 ± 1	47 ± 14
Peptide II	10.5 ± 3.5	69 ± 24	4.5 ± 1.6	53 ± 16

cm^{-1} and 1630 cm^{-1} display a strong contribution from the $\tau_1 = 4$ ps component, which can be seen without numerical analysis by the considerable differences of the transient spectra recorded at 2 and 5 ps, which result in a shift in band position. Finally the bands around 1530 cm^{-1} decay with $\tau_2 = 12.5$ ps. Apparently, the bands around 1530 and 1630 cm^{-1} are due to vibrational modes in the excited electronic state and reflect changes in both the excited state and its decay. These results are in good agreement with the visible data showing that the isomerization reaction is completed with the $\tau_2^{\text{VIS}} = 13$ ps component.

Peptide I. At the position of the ground-state vibrational bands of the pHTI switch, optical excitation leads to a strong absorption decrease. Again there is a strong induced absorption in the 1530 cm^{-1} range (Figure 6b), as observed for pHTI. An important feature is observed in the range of the amide I band: immediately after optical excitation of the chromophore, there is a strong bleach (absorption decrease) at 1640 cm^{-1} and 1670 cm^{-1} , at positions where the original chromophore pHTI does not absorb. At very late delay times, the absorption changes recover toward the stationary absorption difference spectrum (see Figures 6b and 7b). In Peptide I, the contribution of the 5.5 ps kinetic component are somewhat smaller than those observed in the chromophore pHTI.

mHTI. The essential features observed in the IR after optical excitation (see Figures 8a and 7c) are similar to those observed in pHTI. The observed time constant τ_2 is somewhat larger, and the value $\tau_2 = 51$ ps found in the visible experiment can also be used to model the IR data. In mHTI, the contribution of the $\tau_1 = 3.5$ ps component is clearly seen since the shape of the 1530 cm^{-1} band strongly changes during the first 20 ps.

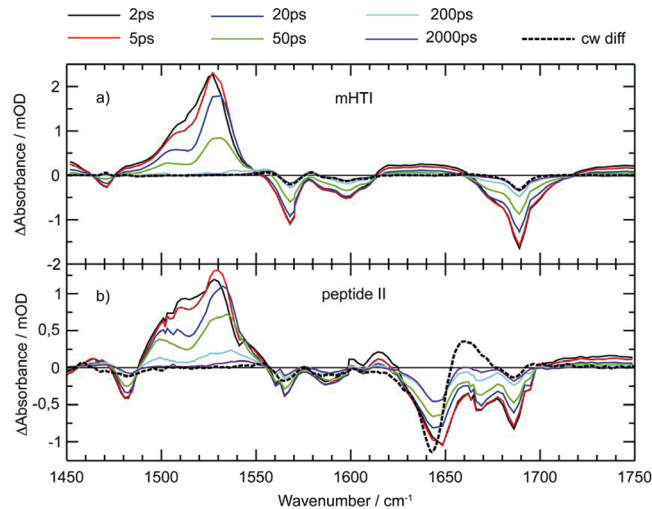


Figure 8. Transient absorption spectra recorded for the delay times given in the upper part of the figure for mHTI (a) and Peptide II (b). The dashed curves give the stationary difference spectra, scaled to fit the amplitudes of the transient absorption change of the band around 1685 cm^{-1} at late delay times.

Apparently there is a band in the 1515 cm^{-1} range that strongly loses amplitude with the τ_1 process.

Peptide II. At early times, the absorption difference spectrum of Peptide II (see Figure 8b) features the absorption reduction of the ground-state bands of the chromophore, the excited-state absorption, and strongly reduced absorption in the amide I range at 1645 cm^{-1} and 1670 cm^{-1} . At later times, the absorption changes essentially follow the $\tau_2 = 53$ ps time constant related to the decay of the excited electronic state. In the 1510 cm^{-1} range, a pronounced contribution from the τ_1 component is visible. At late delay times ($t_D = 200$ ps, see Figure 8b), the absorption change in the chromophore bands is comparable to those of the pure chromophore. However, a strong absorption decrease remains in the amide I region. This behavior is clearly seen in Figures 8b and 7d, where the very late absorption changes ($t_d = 2000$ ps) are plotted together with the stationary difference spectrum in an enlarged scale. Please note that the two spectra are scaled relative to each other for equal amplitudes of the C=O band of the mHTI switch at 1685 cm^{-1} . While the absorption difference spectrum of Peptide I at late times is similar to the stationary difference spectrum (see Figure 7b), the situation is completely different for Peptide II (see Figure 7d): in the range of the amide I band, a strong bleach around 1645 cm^{-1} and increased absorption around 1660 cm^{-1} are present in the stationary spectrum. However, the $t_d = 2000$ ps spectrum shows a much weaker 1647 cm^{-1} bleach (only 1/2 to 1/3 of the final bleach), and no absorption increase at 1660 cm^{-1} . Apparently pronounced structural changes occur in Peptide II after the end of our observation period on the way to the E-form of Peptide II. The observed spectral signatures point to delayed hydrogen bond rupture. Presumably, the conformational freedom of the mHTI chromophore acts as a damper (Scheme 1). It reduces the influence of direct force driven unzipping of hydrogen bonds. The final decrease in hydrogen bonds is only reached much later when the peptide adjusts to the new form of the central part of HTI in thermal reactions.

The experimental observations can be summarized as follows: (i) In all four samples, the kinetic components follow

the reaction scheme known from other HTI compounds. (ii) In the two peptide samples we observe an increased absorption on the red wing of the product band in the visible absorption spectrum at late delay times. (iii) The time constants observed in the visible and in the IR agree well within experimental accuracy. (iv) Compounds containing the para-substituted chromophore react faster than the meta-substituted ones. HTI switches react faster than the related chromo-peptides. (v) The small peptide system, Peptide I, approaches the stationary IR spectrum after the decay of the excited electronic state and hence within our observation window of 3.5 ns. Apparently, no structural changes, which are visible in the IR spectrum, are present on longer time scales. (vi) Peptide II does not reach its stationary E-conformer structure within the 3.5 ns observation period.

4. INTERPRETATION ON A MOLECULAR LEVEL

The Molecular Switches. The time-resolved experiments on the switches pHTI and mHTI reveal two kinetic processes in the 1–100 ps time domain. The slower process can be assigned to the decay of the excited electronic state. This assignment is strongly supported by the spectroscopy with IR probing, which shows that the recovery of the ground-state absorption bands occurs with the time constant τ_2 . After the return to the ground state, a considerable amount of the optical excitation energy is left in the molecule as vibrational excitation. The vibrational relaxation of such a hot ground state is known to take place in the 10 ps range. For pHTI, τ_2 is found in this range. However, the DAS (see Supporting Information) clearly show that only a minor contribution could be due to vibrational cooling. For longer time constants of τ_2 , as found for the peptides, the contributions of vibrational cooling become negligible. The faster kinetic component ($\tau_1 = 6$ ps) displays in the visible spectral range the same spectral features observed previously for other HTI compounds. According to these studies, τ_1 should be related to an excited-state reaction where the charge transfer character of the HTI chromophore is increased. This interpretation is supported by the infrared experiments: with τ_1 we observe strong changes in the excited-state vibrational spectra in the 1510 cm^{-1} range, which reflect changes in the electronic properties of the HTI molecule.

The Peptides. The presented experiments clearly show that the HTI switch is fully active in both peptides. Taking the amplitude of the bleach of the chromophore band in the IR (at ca. 1680 cm^{-1}) at early delay times as a measure for the chromophore excitation, and the amplitude of this bleach at late delay times as a measure for isomerized chromophores, we can use the ratio of the two amplitudes to be proportional to the isomerization yield. Since we find very similar amplitude ratios for all four samples, we conclude that the different substitutions and the incorporation of the HTI in the peptides do not significantly change the isomerization yield. Another striking feature observed in both peptides upon optical excitation of the HTI switch is a rapid decrease in the amide I absorption bands at 1645 cm^{-1} and 1670 cm^{-1} on the subpicosecond time-scale. The instantaneous appearance of this bleach and its subsequent decay (with τ_2) both indicate that the related peptide groups strongly interact with the electronic system of the HTI switch. Since the amino acid attached to the carbonyl function of the thioindigo part of HTI interacts with the π -electron system of the HTI switch, it is evident that this group can be related to the observed instantaneous bleaching.

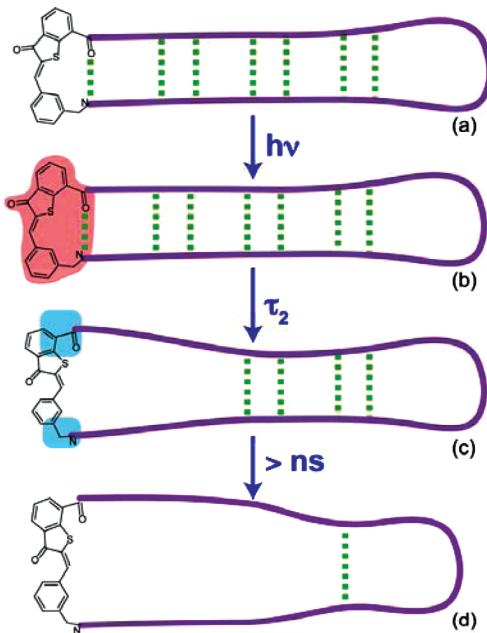
The increase in the τ_2 time constant from the pure HTI switches in comparison with the peptides, where amino acids are directly bound to the switches, can be explained by two alternatives: (i) The peptide attached to the HTI switch will impose friction on the isomerizing motion of the molecular switch. This interaction slows this motion when it occurs on a potential surface with small gradients. (ii) The binding of the peptide groups at the carbonyl and amino function of the HTI switch directly changes the reaction speed of the HTI switch as presented in former publications. It is well-known that electron donating or withdrawing groups strongly influence the potential energy landscape in the vicinity of the transition region on the excited electronic state. The reduction of electron donating power on the stilbene part by the formation of the amide bond as well as the reduction of electron withdrawing power by the formation of the amide bond on the thioindigo part are both expected to increase the barrier height in the excited electronic state. Consequently, this decreases the isomerization speed and hence the decay of the excited electronic state. This behavior has also been described in the literature. On the other hand, experiments of HTI compounds in highly viscous solvents revealed only a small influence on the reaction speed [T. T. H. Herzog, T. Cordes, W. Zinth, unpublished results]. From these observations, we conclude that the deceleration of the decay of the excited electronic state in the two peptides is essentially due to the change in electron donating and withdrawing power at the hemistilbene and hemithioindigo parts, respectively, and hence due to the linkage to the amide-bonds.

In both peptide systems, transient visible spectroscopy on the 100 ps time scale reveals an absorption increase in the red wing of the E-absorption band. This feature can be explained in a similar way as related absorption changes observed in azobenzene peptides.^{4,6–10,50} After isomerization of the molecular switch, the attached peptide does not complete its structural rearrangement within the short isomerization time of the molecular switch. Since larger molecular groups have to be transferred through the viscous solvent surroundings in both peptides, some strain remains on the 100 ps time scale between the peptide moiety and the molecular switch. This strain keeps the chromophore away from its minimum on the ground state potential energy surface of the E-form during the picosecond time domain. The minimum is gradually reached when the peptide moiety approaches its stationary structure in slower thermal steps. The deviation from the minimum of the potential energy surface is connected with a red shift of the absorption band or an increased red wing absorption. Since the IR measurements clearly show that the structural rearrangement of Peptide II is not finished within our observation time of a few nanoseconds, the existence of an additional band in the long time visible absorption spectrum is not surprising. It may account for mHTI molecules in an unrelaxed geometry.

The combined investigation of different meta- and para-substituted HTI amino acids and chromopeptides with ultrafast spectroscopy in the visible and infrared spectral range convincingly showed that (i) HTI chromophores are well suited to be used as ultrafast light-operated switches of peptide conformations and that (ii) long lasting, large scale structural changes occur in Peptide II. (iii) In this β -hairpin model system, strongly driven structural changes on the 70 ps time scale are followed by much slower conformational changes. (iv) Long-time absorption changes in the IR spectrum point to a disruption of interstrand hydrogen bonds and a (partial) disassembly of the β -hairpin structure after switching of the

HTI chromophore. The sequence of molecular processes induced by the optical switching of the chromophore mHTI of Peptide II is visualized in Scheme 2: Prior to optical switching,

Scheme 2. Schematic Presentation of the Structural Dynamics of Peptide II Observed upon Light-Switching of the Chromophore mHTI^a



^aThe solid line represents the backbone of the peptide; the dashed lines represent possible interstrand hydrogen bonds. (a) Starting structure. (b) Electronic excitation of the mHTI changes the electronic system (red area) of the chromophore, which may extend towards the attached peptide and influences the IR-absorption of amide groups. (c) Immediately after isomerization of the mHTI, the system stays in a structure where the peptide part is not yet in its equilibrium structure. The equilibrium structure is only reached on a longer time scale of >3 ns (d).

mHTI is in the Z-form, and the peptide forms at the β -hairpin structure with several (ca. 7) interstrand hydrogen bonds (Scheme 2a). Immediately after light absorption, mHTI is in the excited electronic state, and the changed π electron system leads to bleaching of amide I absorption in close vicinity to the mHTI (Scheme 2b). Directly after the decay of the excited electronic state and the isomerization, the switch mHTI is in a distorted E-form. At this time, the new geometry of mHTI can only fit to the peptide if hydrogen bonds in the β -hairpin structure are broken (Scheme 2c). The conformational freedom of mHTI and the peptide strand prevent the destruction of the complete β -hairpin on the picosecond time scale. Only hydrogen bonds close to the mHTI switch are broken in this process. However, the system has not yet reached its equilibrium structure. The relaxation toward the stationary structure (Scheme 2 d) in slower, thermally driven allosteric rearrangements finally lead to a structure with few interstrand hydrogen bonds. The large Peptide II displays a hierarchy of dynamics that is different from the one observed during unfolding of the light-switchable (noncyclic) β -hairpin model peptide AzoTrpZip2, where the azobenzene switch forms the variable loop element. For AzoTrpZip2, time-resolved IR spectroscopy reveals that destruction of hydrogen bonds, i.e.,

hairpin unfolding, is essentially finished on the picosecond time scale.

ASSOCIATED CONTENT

Supporting Information

The Supporting Information contains more detailed information on the photostationary states, IR-difference spectra, absorption transients at selected probing wavelengths, and decay associated IR spectra. This information is available free of charge via the Internet at <http://pubs.acs.org>.

AUTHOR INFORMATION

Corresponding Author

*E-mail: karola.rueck-braun@tu-berlin.de (K.R.-B.); wolfgang.zinth@physik.uni-muenchen.de (W.Z.).

Author Contributions

#Contributed equally to the present publication.

Notes

The authors declare no competing financial interest.

ACKNOWLEDGMENTS

The authors thank the Deutsche Forschungsgemeinschaft (Excellence Cluster CIPSM, Excellence Cluster 314 (KRB) and SFB 749) and the Volkswagen-Foundation for financial support.

REFERENCES

- Buchner, J.; Kieflhaber, T. *Protein Folding Handbook*, 1st ed.; Wiley-VCH Verlag: Weinheim, Germany, 2005; Vol. 1–5.
- Dill, K. A.; Ozkan, S. B.; Shell, M. S.; Weikl, T. R. *Annu. Rev. Biophys.* **2008**, *37*, 289–316.
- Cui, Q.; Karplus, M. *Protein Sci.* **2008**, *17*, 1295–1307.
- Bredenbeck, J.; Helbing, J.; Behrendt, R.; Renner, C.; Moroder, L.; Wachtveitl, J.; Hamm, P. *J. Phys. Chem. B* **2003**, *107*, 8654–8660.
- Bredenbeck, J.; Helbing, J.; Sieg, A.; Schrader, T.; Zinth, W.; Renner, C.; Behrendt, R.; Moroder, L.; Wachtveitl, J.; Hamm, P. *Proc. Natl. Acad. Sci. U.S.A.* **2003**, *100*, 6452–6457.
- Hamm, P.; Lim, M.; DeGrado, W. F.; Hochstrasser, R. M. *J. Chem. Phys.* **2000**, *112*, 1907–1916.
- Satzger, H.; Root, C.; Renner, C.; Behrendt, R.; Moroder, L.; Wachtveitl, J.; Zinth, W. *Chem. Phys. Lett.* **2004**, *396*, 191–197.
- Schrader, T. E.; Schreier, W. J.; Cordes, T.; Koller, F. O.; Babitzki, G.; Denschlag, R.; Renner, C.; Loweneck, M.; Dong, S.-L.; Moroder, L.; Tavan, P.; Zinth, W. *Proc. Natl. Acad. Sci. U.S.A.* **2007**, *104*, 15729–15734.
- Spörlein, S.; Carstens, H.; Satzger, H.; Renner, C.; Behrendt, R.; Moroder, L.; Tavan, P.; Zinth, W.; Wachtveitl, J. *Proc. Natl. Acad. Sci. U.S.A.* **2002**, *99*, 7998–8002.
- Wachtveitl, J.; Spörlein, S.; Satzger, H.; Fonrobert, B.; Renner, C.; Behrendt, R.; Oesterhelt, D.; Moroder, L.; Zinth, W. *Biophys. J.* **2004**, *86*, 2350–2362.
- Fierz, B.; Satzger, H.; Root, C.; Gilch, P.; Zinth, W.; Kieflhaber, T. *Proc. Natl. Acad. Sci. U.S.A.* **2007**, *104*, 2163–2168.
- Bieri, O.; Kieflhaber, T. *Biol. Chem.* **1999**, *380*, 923–929.
- Kubelka, J.; Hofrichter, J.; Eaton, W. A. *Curr. Opin. Struct. Biol.* **2004**, *14*, 76–88.
- Clementi, C. *Curr. Opin. Struc. Biol.* **2008**, *18*, 10–15.
- Denschlag, R.; Schreier, W. J.; Rieff, B.; Schrader, T. E.; Koller, F. O.; Moroder, L.; Zinth, W.; Tavan, P. *Phys. Chem. Chem. Phys.* **2010**, *12*, 6204–6218.
- Zinth, W.; Wachtveitl, J. Light-Triggered Peptide Dynamics. In *Protein Folding and Misfolding, Shining Light by Infrared Spectroscopy*; Fabian, H., Naumann, D., Ed.; Springer-Verlag: Berlin Heidelberg, 2011; pp 171–192.

- (17) Cattani-Scholz, A.; Renner, C.; Cabrele, C.; Behrendt, R.; Oesterhelt, D.; Moroder, L. *Angew. Chem., Int. Ed.* **2002**, *41*, 289.
- (18) Kramer, R. H.; Fortin, D. L.; Trauner, D. *Curr. Opin. Neurobiol.* **2009**, *19*, 544–552.
- (19) Renner, C.; Moroder, L. *ChemBioChem* **2006**, *7*, 869–878.
- (20) Dhawale, A. K.; Hagiwara, A.; Bhalla, U. S.; Murthy, V. N.; Albeau, D. F. *Nat. Neurosci.* **2010**, *13*, 1404–U1183.
- (21) Llewellyn, M. E.; Thompson, K. R.; Deisseroth, K.; Delp, S. L. *Nat. Med.* **2010**, *16*, 1161–U1144.
- (22) Hoppmann, C.; Schmieder, P.; Domaing, P.; Vogelreiter, G.; Eichhorst, J.; Wiesner, B.; Morano, I.; Rück-Braun, K.; Beyermann, M. *Angew. Chem., Int. Ed.* **2011**, *50*, 7699–7702.
- (23) Gorostiza, P.; Volgraf, M.; Numano, R.; Szobota, S.; Trauner, D.; Isacoff, E. Y. *Proc. Natl. Acad. Sci. U.S.A.* **2007**, *104*, 10865–10870.
- (24) Herre, S.; Schadendorf, T.; Ivanov, I.; Herrberger, C.; Steinle, W.; Rück-Braun, K.; Preissner, R.; Kuhn, H. *ChemBioChem* **2006**, *7*, 1089–1095.
- (25) Deeg, A. A.; Schrader, T. E.; Kempfer, S.; Pfizer, J.; Moroder, L.; Zinth, W. *ChemPhysChem* **2011**, *12*, 559–562.
- (26) Nägele, T.; Hoche, R.; Zinth, W.; Wachtveitl, J. *Chem. Phys. Lett.* **1997**, *272*, 489–495.
- (27) Beharry, A. A.; Wong, L.; Tropepe, V.; Woolley, G. A. *Angew. Chem., Int. Ed.* **2011**, *50*, 1325–1327.
- (28) Boulegue, C.; Loewenbeck, M.; Renner, C.; Moroder, L. *ChemBioChem* **2007**, *8*, 591–594.
- (29) Draxler, S.; Brust, T.; Malkmus, S.; Koller, F. O.; Heinz, B.; Laimgruber, S.; Schulz, C.; Dietrich, S.; Rück-Braun, K.; Zinth, W.; Braun, M. *J. Mol. Liq.* **2008**, *141*, 130–136.
- (30) Matsuda, K.; Irie, M. *J. Photochem. Photobiol. C: Photochem. Rev.* **2004**, *5*, 169–182.
- (31) Böttcher, C.; Zeyat, G.; Ahmed, S. A.; Irran, E.; Cordes, T.; Elsner, C.; Zinth, W.; Rueck-Braun, K. *Beilstein J. Org. Chem.* **2009**, *5*, 25.
- (32) Moine, B.; Rehault, J.; Aloise, S.; Micheau, J. C.; Moustrou, C.; Samat, A.; Poizat, O.; Buntinx, G. *J. Phys. Chem. A* **2008**, *112*, 4719–4726.
- (33) Schadendorf, T.; Hoppmann, C.; Rueck-Braun, K. *Tetrahedron Lett.* **2007**, *48*, 9044–9047.
- (34) Steinle, W.; Rück-Braun, K. *Org. Lett.* **2003**, *5*, 141–144.
- (35) Cordes, T.; Schadendorf, T.; Priewisch, B.; Rück-Braun, K.; Zinth, W. *J. Phys. Chem. A* **2008**, *112*, 581–588.
- (36) Cordes, T.; Schadendorf, T.; Rück-Braun, K.; Zinth, W. *Chem. Phys. Lett.* **2008**, *455*, 197–201.
- (37) Cordes, T.; Weinrich, D.; Kempa, S.; Riessmann, K.; Herre, S.; Hoppmann, C.; Rück-Braun, K.; Zinth, W. *Chem. Phys. Lett.* **2006**, *428*, 167–173.
- (38) Cordes, T.; Elsner, C.; Herzog, T. T.; Hoppmann, C.; Schadendorf, T.; Summerer, W.; Rück-Braun, K.; Zinth, W. *Chem. Phys.* **2009**, *358*, 103–110.
- (39) Klare, J. P.; Bordignon, E.; Engelhard, M.; Steinhoff, H.-J. *Eur. J. Cell. Biol.* **2011**, *90*, 731–739.
- (40) Hoppmann, C.; Seedorff, S.; Richter, A.; Fabian, H.; Schmieder, P.; Rück-Braun, K.; Beyermann, M. *Angew. Chem., Int. Ed.* **2009**, *48*, 6636–6639.
- (41) Becker, C. F. W.; Hunter, C. L.; Seidel, R.; Kent, S. B. H.; Goody, R. S.; Engelhard, M. *Proc. Natl. Acad. Sci. U.S.A.* **2003**, *100*, 5075–5080.
- (42) Huber, R.; Satzger, H.; Zinth, W.; Wachtveitl, J. *Opt. Commun.* **2001**, *194*, 443–448.
- (43) Schrader, T.; Sieg, A.; Koller, F.; Schreier, W.; An, Q.; Zinth, W.; Gilch, P. *Chem. Phys. Lett.* **2004**, *392*, 358–364.
- (44) Cordes, T.; Heinz, B.; Regner, N.; Hoppmann, C.; Schrader, T. E.; Summerer, W.; Rück-Braun, K.; Zinth, W. *ChemPhysChem* **2007**, *8*, 1713–1721.
- (45) Nenov, A.; Cordes, T.; Herzog, T. T.; Zinth, W.; de Vivie-Riedle, R. *J. Phys. Chem. A* **2010**, *114*, 13016–13030.
- (46) Rück-Braun, K.; Kempa, S.; Priewisch, B.; Richter, A.; Seedorff, S.; Wallach, L. *Synthesis* **2009**, 4256–4267.
- (47) Barth, A.; Zscherg, C. *Q. Rev. Biophys.* **2002**, *35*, 369–430.
- (48) Schrader, T. E.; Cordes, T.; Schreier, W. J.; Koller, F. O.; Dong, S. L.; Moroder, L.; Zinth, W. *J. Phys. Chem. B* **2011**, *115*, 5219–5226.
- (49) Tremmel, S.; Beyermann, M.; Oschkinat, H.; Bienert, M.; Naumann, D.; Fabian, H. *Angew. Chem., Int. Ed.* **2005**, *44*, 4631–4635.
- (50) Bredenbeck, J.; Helbing, J.; Kumita, J. R.; Woolley, G. A.; Hamm, P. *Proc. Natl. Acad. Sci. U.S.A.* **2005**, *102*, 2379–2384.